William G. Bradley, Jr, MD, PhD

MR Appearance of Hemorrhage in the Brain[1]

The appearance of intracranial hemorrhage at magnetic resonance (MR) imaging depends primarily on the age of the hematoma and the type of MR contrast (ie, T1 or T2 weighted). As a hematoma ages, the hemoglobin passes through several forms (oxyhemoglobin, deoxyhemoglobin, and methemoglobin) prior to red cell lysis and breakdown into ferritin and hemosiderin. Five distinct stages of hemorrhage can be defined: hyperacute (intracellular oxyhemoglobin, long T1 and T2), acute (intracellular deoxyhemoglobin, long T1, short T2), early subacute (intracellular methemoglobin, short T1, short T2), late subacute (extracellular methemoglobin, short T1, long T2), and chronic (ferritin and hemosiderin, short T2). The short T1 of methemoglobin is due to the paramagnetic dipole-dipole interaction. Another paramagnetic property, the magnetic susceptibility effect, is responsible for the short T2 observed when deoxyhemoglobin, methemoglobin, or hemosiderin is intracellular. T2 shortening can also be produced by hemoconcentration and clot retraction. The T2 shortening due to magnetic susceptibility effects is enhanced on higher-field-strength systems and on gradient-echo images and is reduced with "fast spin-echo" MR techniques.

Index terms: Brain, hemorrhage, 10.367 • Brain, MR, 10.1214 • State-of-art reviews

Radiology 1993; 189:15–26

THE appearance at magnetic resonance (MR) imaging of most lesions in the brain has a direct correlate in computed tomography (CT). Most lesions, being edematous, appear dark on both unenhanced CT scans and T1-weighted MR images (ie, those acquired with a short repetition time [TR] [approximately 500 msec] and a short echo time [TE] [approximately 20 msec] in which T1 contrast predominates). Such lesions also appear bright on T2-weighted MR images (ie, those acquired with a long TR [approximately 3,000 msec] and a long TE [approximately 80 msec] in which T2 contrast predominates). Hemorrhage, on the other hand, may be bright or dark on T1- or T2-weighted images, depending on the *age* of the hematoma and the integrity of the red blood cell membrane (1–7). The combination of appearances on T1- and T2-weighted images defines five stages of hemorrhage that can be distinguished with MR imaging (Table).

Much of what has been written on the MR appearance of hemorrhage is contradictory and confusing. Some have suggested that there is no predictable temporal pattern of hemoglobin oxidation (8). Some accept the appearance but have questioned the specific mechanism (9–11). The purpose of this review is to describe the *usual* pattern of evolving hemorrhage, the proposed mechanisms behind the changes, and the technical factors that affect the MR appearance.

On CT scans, acute intracranial hemorrhage usually becomes hyperattenuating within an hour as the clot retracts. This lasts for several days, and then the hemorrhage fades to become isoattenuating and, eventually, hypoattenuating. On MR images, hemorrhage less than 12 hours old may not be distinguishable from any other edematous mass. Thus, CT should be used to detect hemorrhage in the brain during the first 12 hours after ictus. The subsequent MR appearance of hemorrhage (Table) is an evolving pattern of variable signal intensity that depends on the specific form of hemoglobin present (ie, oxyhemoglobin, deoxyhemoglobin, or methemoglobin) (Fig 1), on whether the red blood cells are intact or lysed, on the operating field strength and the receiver bandwidth, on the type of signal (that is, routine spin echo [SE], fast SE, or gradient echo [GRE]), and on the degree of T1 or T2 weighting (7).

The appearance of hemorrhage depends on the specific intracranial compartment involved: subarachnoid, intraventricular, subdural, epidural, intratumoral, or intraparenchymal. Different zones may also be defined from the inner core to the outer rim of parenchymal hematomas. Because there are unpaired electrons in the heme iron of deoxyhemoglobin and methemoglobin, some basic concepts of paramagnetism must be understood in order to appreciate fully the different T1 and T2 characteristics. Paramagnetic phenomena such as the "electron-proton dipole-dipole interaction" and "magnetic susceptibility effects" both enter into a discussion of the MR appearance of hemorrhage.

PARAMAGNETISM IN HEMORRHAGE

There are two primary mechanisms for T1 and T2 shortening in hemorrhage (Fig 2): "bound-water effects" and "paramagnetic effects" (7,11). Free, "bulk-phase" water (such as cerebrospinal fluid [CSF]) has very high natural motional frequencies (or, alternatively, very short molecular correlation times). Because these natural

[1] From the Long Beach Memorial Medical Center, Calif. Received January 22, 1993; revision requested February 25; revision received April 7; accepted April 8. **Address reprint requests to** the author, Memorial Magnetic Resonance Center, 403 E Columbia St, Long Beach, CA 90806.

Abbreviations: CSF = cerebrospinal fluid, GRE = gradient echo, SE = spin echo, TE = echo time, TR = repetition time.

Evolution of Parenchymal Hematomas as Seen at MR Imaging

Stage	Age	Compartment	Hemoglobin	Intensity Compared to Brain: T1-weighted Image	Intensity Compared to Brain: T2-weighted Image
Hyperacute	<24 h	Intracellular	Oxyhemoglobin	Isointense	Slightly hyperintense
Acute	1–3 d	Intracellular	Deoxyhemoglobin	Slightly hypointense	Very hypointense
Subacute					
Early	>3 d	Intracellular	Methemoglobin	Very hyperintense	Very hypointense
Late	>7 d	Extracellular	Methemoglobin	Very hyperintense	Very hyperintense
Chronic	>14 d	Extracellular	Hemichromes	Isointense	Slightly hyperintense
Center					
Rim		Intracellular	Hemosiderin	Slightly hypointense	Very hypointense

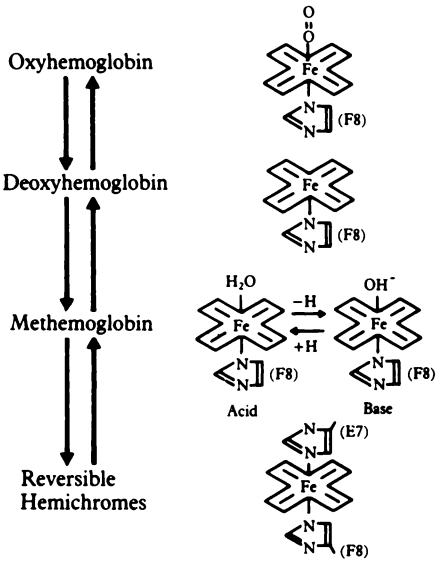

Figure 1. Oxidative denaturation of hemoglobin. In the circulating form, hemoglobin goes between the oxy state (as it leaves the pulmonary circulation) and the deoxy state (as it leaves the capillary circulation). Although there is a higher concentration of deoxyhemoglobin in venous blood (30%) compared with arterial blood (5%), oxyhemoglobin is the predominant form throughout the circulation. The heme iron in both oxy- and deoxyhemoglobin is in the ferrous (Fe^{2+}) state. The heme iron in the oxy form is diamagnetic, that is, it has no unpaired electrons and, therefore, exhibits no paramagnetism. There are four unpaired electrons on the heme iron in deoxyhemoglobin, which is, therefore, paramagnetic. When the hemoglobin is removed from the high oxygen environment of the circulation, the heme iron undergoes oxidative denaturation to the ferric (Fe^{3+}) state, forming methemoglobin. The combination of five unpaired electrons on the heme iron and a water molecule at the sixth coordination site (in the acid form, which predominates at physiologic pH) results in T1 shortening. Continued oxidative denaturation forms low-spin (diamagnetic) ferric hemichromes where the sixth coordination site is occupied by a second histidine group from the now-denatured globin chain. (Reprinted, with permission, from reference 12.)

motional frequencies are much higher than the Larmor frequencies used in MR imaging, T1 relaxation is inefficient and the T1 relaxation time of CSF is longer than that of any other substance in the body (approximately 2,700 msec) (11).

When protein is added to pure water, the polar water molecules are attracted or "bound" to the charged side groups of the protein, forming a hydration layer. Water in this hydration layer environment has longer molecular correlation times and shorter T1 relaxation times than pure CSF (ie, approximately 400–1,000 msec, depending on protein concentration). Thus the T1 of nonparamagnetic, proteinaceous oxyhemoglobin is much less than that of CSF and approaches that of brain parenchyma (11).

Considerably greater T1 shortening is possible due to the dipole-dipole interaction resulting from paramagnetic substances such as gadolinium or methemoglobin in aqueous solution. Such paramagnetic substances (13) (defined by the presence of unpaired electrons) may shorten the T1 of aqueous solutions into the several hundred millisecond range, which is considerably shorter than that possible with diamagnetic species (ie, those *not* having unpaired electrons).

A similar statement can be made for T2 shortening. Proteinaceous solutions of sufficient concentration can bind sufficient water to cause observable T2 shortening compared with that of brain. Such "solutions" are really more like mucinous gels (11) and contribute to the T2 shortening observed at high hematocrit as water is resorbed from a hematoma (7). Substantially greater T2 shortening is observed from the magnetic susceptibility effects resulting from compartmentalization of paramagnetic deoxy- or methemoglobin inside intact red blood cells (7). In general, the greater the number of unpaired electrons, the greater the paramagnetic effect (14).

Because the interaction between the dipole of the unpaired electrons and that of a hydrogen nucleus falls off as the sixth power of the distance between them, hydrogen nuclei must be able to approach the paramagnetic center within a distance of 3 Å (13), or there will be negligible T1 shortening. In methemoglobin the water molecules can closely approach the heme iron, but in deoxyhemoglobin they cannot because of the configuration of the protein. Therefore, methemoglobin demonstrates paramagnetic T1 shortening but deoxyhemoglobin does not.

Paramagnetic substances also become more strongly magnetized than diamagnetic substances when placed in a magnetic field. Exactly *how* magnetized a substance becomes is quantified by the magnetic susceptibility coefficient, which is the ratio of the induced to the applied magnetic field. Paramagnetic substances such as hemosiderin have high magnetic susceptibilities and become more magnetized than diamagnetic substances when placed in an external magnetic field. This leads to focal "hot spots," which create local regions of magnetic nonuniformity. These in turn lead to rapid dephasing of spins and signal loss on T2*-weighted *GRE* images (14–18). As water protons diffuse through these magnetically nonuniform regions, they lose phase coherence in proportion to the interecho time, which also decreases the signal intensity on T2-weighted *SE* images (1,17,19). Because the induced field (and thus the induced nonuniformity) is proportional to the strength of the applied magnetic field (through the magnetic susceptibility coefficient), both T2* and T2 shortening are greater at higher field strengths (1,5,15). To the extent that dephasing results from diffusion through the field gradients (20) resulting from these nonuniformities, T2 decreases as the square of the field strength (1) at constant bandwidth. As the receiver bandwidth is decreased on systems of low and middle field strength, however, the sensitivity to susceptibility effects is increased somewhat, partially reflecting the longer TEs required to accommodate the longer echo sampling times. As the time available for diffusion decreases—for example, with the short echo spacing of "fast SE"—the sensitivity to this magnetic susceptibility decreases (21,22), although some workers main-

T1 Shortening

Marked: Dipole-dipole interaction (eg, methemoglobin)
Mild: Hydration layer water (eg, proteinaceous serum)

T2 Shortening

Field-strength dependent (marked):
- Magnetic susceptibility effects (eg, intracellular deoxyhemoglobin and methemoglobin)
- Hydration layer water (eg, increasing hematocrit)

Field-strength independent (mild):
- Fibrin clot formation
- Fibrin clot retraction
- Red blood cell dehydration

Figure 2. Mechanisms of T1 and T2 shortening in hemorrhage.

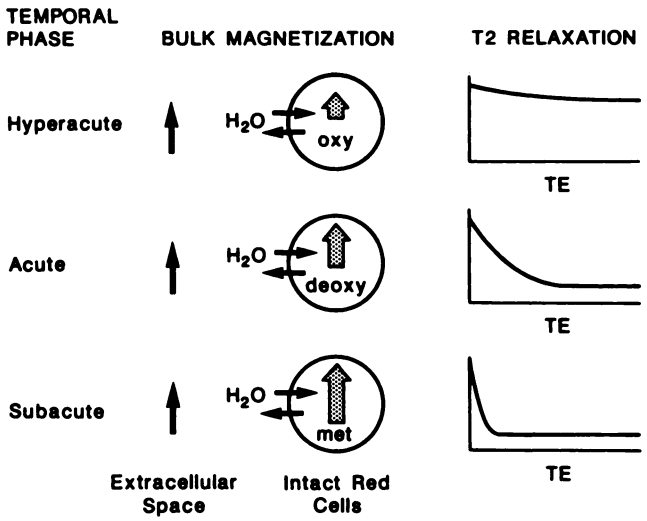

Figure 3. T2 shortening in fresh hematomas. T2 relaxation time of a hematoma depends on its temporal phase (hyperacute: first few hours; acute: 1–3 days; subacute: > 3 days). In all phases, bulk magnetization of the extracellular space is the same (arrow of constant size). Bulk magnetization of the intracellular compartment (within intact red blood cells) changes during the evolution of the hematoma. Oxyhemoglobin (during the hyperacute phase) has low induced magnetization because of its low magnetic susceptibility. This results in similar induced magnetization in the intracellular and extracellular environments such that water diffusing across the red blood cell membrane experiences a constant field. For this reason, there is no dephasing due to diffusion and therefore little T2 relaxation. During the acute phase, magnetically susceptible deoxyhemoglobin is formed, resulting in a higher magnetization within the red blood cell than in the surrounding extracellular space. The magnetic field gradient experienced by water molecules diffusing across the red blood cell membrane results in additional dephasing and T2 shortening. Since the red cells are still intact during the early subacute phase when methemoglobin is formed, even greater dephasing will occur due to the somewhat higher magnetization induced in methemoglobin with five unpaired electrons compared to deoxyhemoglobin, which has four.

tain that this decrease is not significant (23). To summarize, the sensitivity to the magnetic susceptibility effects of hemorrhage increase as one progresses from fast SE to routine SE to GRE techniques, from T1 to T2 (or T2*) weighting, from short to long interecho times or echo spacing, and from lower to higher field strengths.

Dephasing can also result from the diffusion of water molecules across red blood cell membranes when the magnetic susceptibility inside the red blood cell differs from that outside (Fig 3) (20). For example, when paramagnetic deoxyhemoglobin or methemoglobin is present within intact red blood cells in an acute or early subacute hematoma, the induced magnetic field inside the red blood cell is much greater than that outside in the nonparamagnetic plasma. Water molecules diffusing across the red cell membrane thus experience a magnetic field gradient, which results in dephasing and T2 shortening (Fig 3).

Clot retraction also causes T2 shortening (24–27). Since this effect does not depend on field strength, it contributes more to the observed T2 shortening at lower field strengths than at higher field strengths. Patients with hemorrhagic diatheses or those receiving anticoagulants, therefore, may not demonstrate the expected T2 shortening following acute hemorrhage, particularly when imaged at lower field strengths.

OXIDATION OF HEMOGLOBIN

The variable MR appearance of hemorrhage (Fig 4) depends on the structure of hemoglobin and its various oxidation products (28) (Fig 1). In the circulation, hemoglobin alternates between the oxy and deoxy forms. As the blood passes through the high oxygen environment of the lungs, molecular oxygen (O_2) is bound, forming oxyhemoglobin. When the blood then passes through the lower oxygen environment of the capillaries, the O_2 is given off, forming deoxyhemoglobin. To bind oxygen reversibly, the iron in the hemoglobin (the "heme iron") must be maintained in the reduced, ferrous (Fe^{2+}) state. When the red blood cell is removed from the high oxygen environment of the circulation, deoxyhemoglobin undergoes denaturation to methemoglobin, and the heme iron becomes oxidized to the ferric (Fe^{3+}) form.

Changes in the conformation of the hemoglobin molecule result from changes in the oxidation state of the heme iron. The heme iron is normally held in a nonpolar crevice in the hemoglobin molecule. It is held by a covalent bond to a histidine attached at the F8 position of the globin chain and by four hydrophobic van der Waals forces to nonpolar groups on the globin molecule. The sixth coordination site of the heme iron is occupied by molecular oxygen in oxyhemoglobin and is vacant in deoxyhemoglobin (Fig 1). In methemoglobin, the sixth coordination site is occupied by either a water molecule or a hydroxyl ion, depending on whether the methemoglobin is in the acid or base form, respectively (6). At physiologic pH, the acid form predominates. With continued oxidative denaturation, methemoglobin is converted to derivatives known as hemichromes (28). The iron in these compounds remains in the ferric state. An alteration of the tertiary structure of the globin molecule occurs such that the sixth coordination site of the heme iron becomes occupied by a ligand

from within the globin molecule (the distal histidine at E7).

After red blood cell lysis, the hemoglobin is broken down into the heme iron and the globin molecule. The iron is initially stored as ferritin, which is water-soluble ferric hydroxide-phosphate micelles attached to the iron storage protein, apoferritin (29,30). With localized iron overload (13) and depletion of apoferritin, hemosiderin is formed, which represents water-insoluble clumps of ferritin particles (29).

While the oxidation state of the heme iron has everything to do with its function, it has nothing at all to do with the appearance of blood on MR images. The MR appearance depends on whether there are unpaired electrons, that is, on whether the species is paramagnetic. The magnetic properties of hemoglobin were initially described almost 150 years ago by Faraday (31) and subsequently by Pauling and Coryell (32). Basically, oxyhemoglobin and the hemichromes are diamagnetic—that is, they have no unpaired electrons—and deoxy- and methemoglobin are paramagnetic. Deoxyhemoglobin has four unpaired electrons and methemoglobin has five. Since seven unpaired electrons is the maximum possible (eg, gadolinium), deoxy- and methemoglobin are, indeed, quite paramagnetic.

Paramagnetism per se does not ensure T1 shortening in aqueous solution; the paramagnetic centers must also be accessible to surrounding water protons. Quantitation of T1 shortening requires consideration of the magnitude of the magnetic moment of the paramagnetic dipole (that is, the number of unpaired electrons), the electron spin relaxation time, the concentration of paramagnetic dipoles, the average distance from surrounding water protons, and the relative motions of the protons and the paramagnetic centers (6,13). Theories of proton relaxation by paramagnetic solutes are based on translational diffusion and the distance of closest approach of the proton and paramagnetic ions, which determines an "outer sphere" of influence (33). It has also been shown that there can be a contribution to the relaxation from exchange between the solvent and water ligands in the first coordination sphere of the paramagnetic ion, that is, "inner-sphere effects" (33).

Although deoxyhemoglobin is paramagnetic, it does not cause T1 shortening. Because the electron spin relaxation time of deoxyhemoglobin is very short and because water molecules are unable to approach the heme iron within a distance of 3 Å, the T1 of an aqueous solution of deoxyhemoglobin is not short (34). In fact, the T1 of an acute hematoma is prolonged (compared to brain) due to the higher water content (35). The frequencies corresponding to the electron spin relaxation time of methemoglobin, on the other hand, are much closer to the Larmor frequencies used in MR imaging (32). Also water molecules are better able to approach the paramagnetic center in methemoglobin than in deoxyhemoglobin (33). Thus, methemoglobin causes significant T1 shortening in aqueous solutions, while deoxyhemoglobin does not.

Form of hemoglobin: oxyhemoglobin, deoxyhemoglobin, methemoglobin
Breakdown products of hemoglobin: hemichromes, ferritin, hemosiderin
Red blood cell membrane integrity
Red blood cell dehydration
Hematocrit
Clot formation and retraction
Magnetization transfer effects
Compartment in brain (ambient 0_2 level): parenchymal, intratumoral, subdural, epidural, intraventricular, subarachnoid
MR technique: SE, GRE, fast SE
MR contrast: T1- or T2-weighted
Field strength
Bandwidth

Figure 4. Factors affecting the MR appearance of hemorrhage.

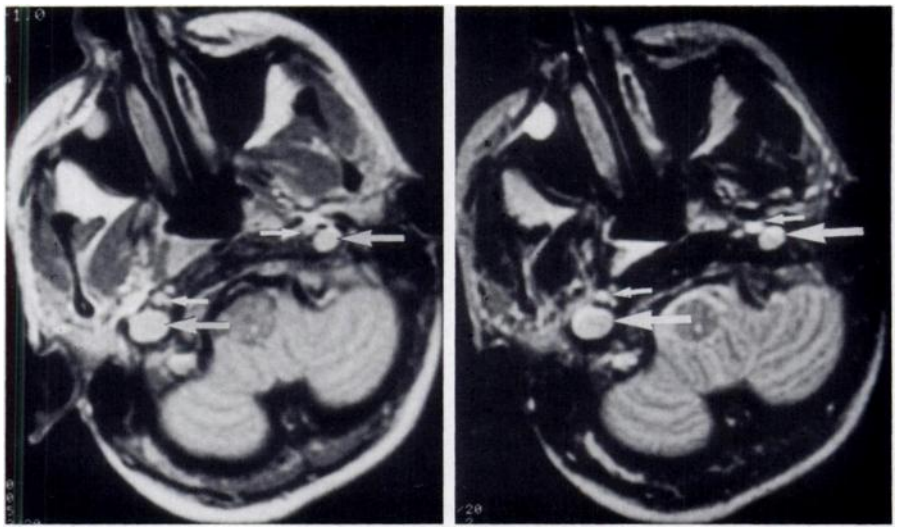

a. b.

Figure 5. Hyperacute hemorrhage (stagnant oxyhemoglobin) in a 35-year-old heroin addict who had experienced cardiopulmonary arrest immediately prior to the acquisition of these images. **(a)** Proton-density–weighted MR image (SE 3,000/25 [TR msec/TE msec]) demonstrates high intravascular signal intensity due to complete absence of motion in the jugular veins (large arrows) and carotid arteries (small arrows). **(b)** T2-weighted (SE 3,000/80) axial MR section through the same level as **a** demonstrates intravascular hyperintensity (arrows) due to long T2 of unclotted intracellular oxyhemoglobin. (The patient was subsequently resuscitated.)

EVOLVING PARENCHYMAL HEMATOMA

For hemorrhage to be staged properly with MR imaging, both T1- and T2-weighted images must be acquired. Five stages of an evolving hematoma can be described (7): hyperacute (intracellular oxyhemoglobin, first few hours), acute (intracellular deoxyhemoglobin, 1–3 days), early subacute (intracellular methemoglobin, about 3–7 days), late subacute (extracellular methemoglobin, more than 7 days), and chronic (older than 2 weeks) (Table).

During the first few hours (hyperacute phase), the hematoma consists of a mixture of oxy- and deoxyhemoglobin (Fig 5), initially as a liquid suspension of intact red blood cells and, as thrombosis progresses and plasma is resorbed, an increasingly solid conglomerate of intact red blood cells (1,25–27). Over the next few days (acute phase), the hematoma consists primarily of deoxyhemoglobin within intact red blood cells (1) (Fig 6). The term "hyperacute" was first adopted

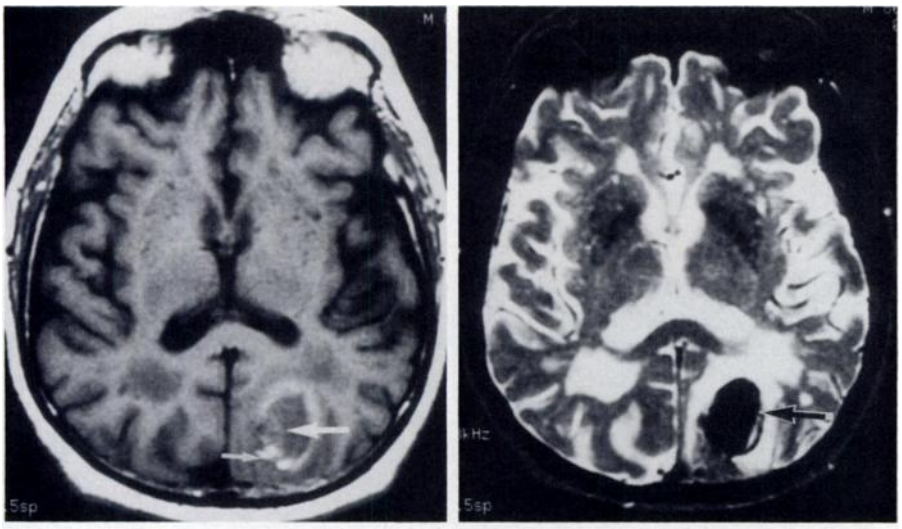

a. b.

Figure 6. Acute hematoma in an 80-year-old man with a 3-day history of "memory loss." **(a)** T1-weighted (SE 500/20) axial MR section demonstrates central area isointense to brain (large arrow) with peripheral rim of hyperintensity (small arrow). **(b)** T2-weighted (SE 3,000/80) axial MR image through the same level as **a** demonstrates marked hypointensity (arrow) on this 1.5-T image. The combination of findings indicates that the hematoma has a markedly shortened T2 with a small peripheral component of shortened T1. The 3-day history and the presence of persistent mass effect and edema indicate that the majority of this hemorrhage is in the intracellular deoxyhemoglobin form with early oxidation to methemoglobin at the periphery.

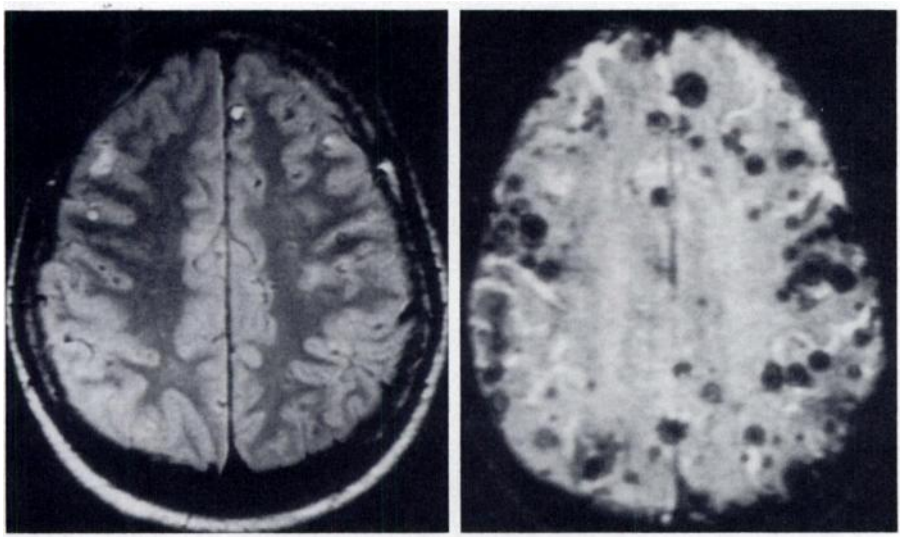

a. b.

Figure 7. Hemorrhagic metastases on high-field-strength, GRE images. This 55-year-old woman presented with headaches without focal neurologic findings. Subsequent work-up revealed hemorrhagic metastases to the brain from small cell carcinoma of the lung. **(a)** Mildly T2-weighted (SE 2,500/30) axial MR section demonstrates a few scattered abnormalities. **(b)** MR image obtained with gradient-recalled acquisition in the steady state (GRE 200/80, 10° flip angle) demonstrates multiple additional foci of low intensity due to additional sensitivity to magnetic susceptibility effects.

(36) to describe the stage preceding deoxyhemoglobin, which was defined as "acute" by Gomori et al (1). Both hyperacute and acute hematomas seen on MR images appear hyperattenuating on CT scans and are labeled "acute."

During the subacute period, which begins after several days, deoxyhemoglobin undergoes oxidative denaturation, forming methemoglobin (6). Early in this phase (Figs 7, 8), the red blood cells are intact. Later in this phase (after approximately 1 week), red cell lysis occurs (Fig 9).

In parenchymal hematomas, modified macrophages (microglia or gitter cells) move in from the periphery by the end of the 2nd week and remove the iron from the extracellular methemoglobin (7). This marks the beginning of the chronic phase when the heme iron is deposited at the periphery as a rim of hemosiderin and ferritin (27) within macrophages (Fig 9) (1). The center of the hematoma is eventually left with non–iron-containing, nonparamagnetic heme pigments, such as hematoidin (37).

A note of caution: Although it is useful to describe the evolution of a hematoma in these well-defined stages, in fact the stages may coexist (8). For example, at the time hemosiderin and ferritin are first deposited at the periphery of a hematoma (indicating the beginning of the chronic stage), free methemoglobin is present in the outer core (late subacute stage) (Fig 9) and intracellular deoxyhemoglobin or even oxyhemoglobin may still be found in the inner core from the acute and hyperacute stages, respectively. By convention, the hematoma is described in terms of the most mature form of hemoglobin that is present (7).

Hyperacute Phase

On short TR/TE, T1-weighted images, hyperacute hematomas (a few hours old) are predominantly oxyhemoglobin and are iso- to hypointense compared with brain due to their longer T1 times, reflecting their higher water content (25–27). The T2 relaxation time reflects both the fluid-solid character of the fresh hematoma (Fig 5) (24–27) and the relative amounts of oxyhemoglobin and deoxyhemoglobin. Ninety-five percent of arterial blood is oxyhemoglobin (29), which is diamagnetic and does not cause T2 shortening. Because most nontraumatic hemorrhages are arterial (such as that from aneurysms, and/or microaneurysms in hypertension), there may be no significant T2 shortening initially (Fig 5). The minimum concentration of deoxyhemoglobin that produces visible T2 shortening depends on the field strength (1), the bandwidth, and the imaging technique, with GRE studies being more sensitive than SE studies (14–18). It should be stressed, however, that during the first few hours after a hemorrhage, MR is less sensitive than CT.

Acute Phase

After the initial 24 hours, deoxyhemoglobin is normally found within clotted, intact red blood cells (1,18). As noted earlier, although deoxyhemoglobin is magnetically susceptible, it

does not cause T1 shortening. T2 shortening results from the dephasing due to diffusion of water molecules in and out of the red blood cell (Fig 6). Since the magnetic susceptibility effects increase with field strength, the low-intensity appearance of an acute hematoma on T2-weighted images may be more obvious at higher field strengths (1). Low flip angle, T2*-weighted, GRE images are also more sensitive to susceptibility effects than T2-weighted SE images (14–18) (Fig 7). Since high field strength and GRE techniques increase the sensitivity to magnetic susceptibility effects through different mechanisms, they are additive (14) and produce marked signal loss when applied together.

During both the hyperacute and acute phases, progressive concentration of red blood cells by thrombosis also causes T2 shortening (Fig 2) (24,26,38,39). This reflects both clot retraction and increasing hematocrit (24,26,27). Formation of the fibrin clot (from polymerization of fibrinogen) and clot retraction (by platelets) both shorten T2 (24). Such effects can be seen in plasma clots alone without any magnetically susceptible species (24). Prior to clot retraction, therefore, T2 shortening may be minimal (25,26).

The T2 shortening that results from increasing hematocrit increases with field strength, like the magnetic susceptibility effects. The mechanism reflects increasing protein concentration and binding of water protons (11,40, 41). T2 shortens progressively as the hematocrit approaches 100% (24). Dehydration of red blood cells is also known to occur during the acute phase and can cause a selective decrease in T2 (42–46).

It should be stressed that it may not be possible to distinguish among the various mechanisms that lead to T2 shortening in acute hemorrhage. Specifically, the signal intensity loss noted in about 24 hours on long TR/TE T2-weighted images may be

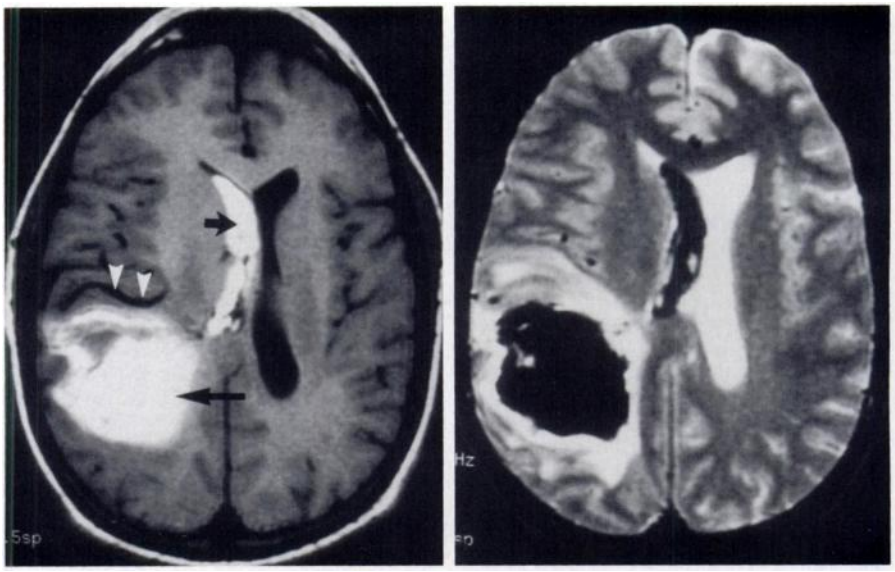

a. b.

Figure 8. Early subacute hematoma in a 30-year-old man with known arteriovenous malformation and 4-day history of obtundation. **(a)** T1-weighted (SE 500/20) axial MR image demonstrates hyperintensity in hematomas within right parietal lobe (large arrow) and right lateral ventricle (small arrow). Note also flow voids of dilated arterial feeders of the arteriovenous malformation (arrowheads). **(b)** T2-weighted (SE 3,000/80) axial MR image demonstrates central hypointensity within both right parietal and right lateral ventricular hematomas. The combination of high signal intensity on the T1-weighted image and low signal intensity on the T2-weighted image is indicative of intracellular methemoglobin.

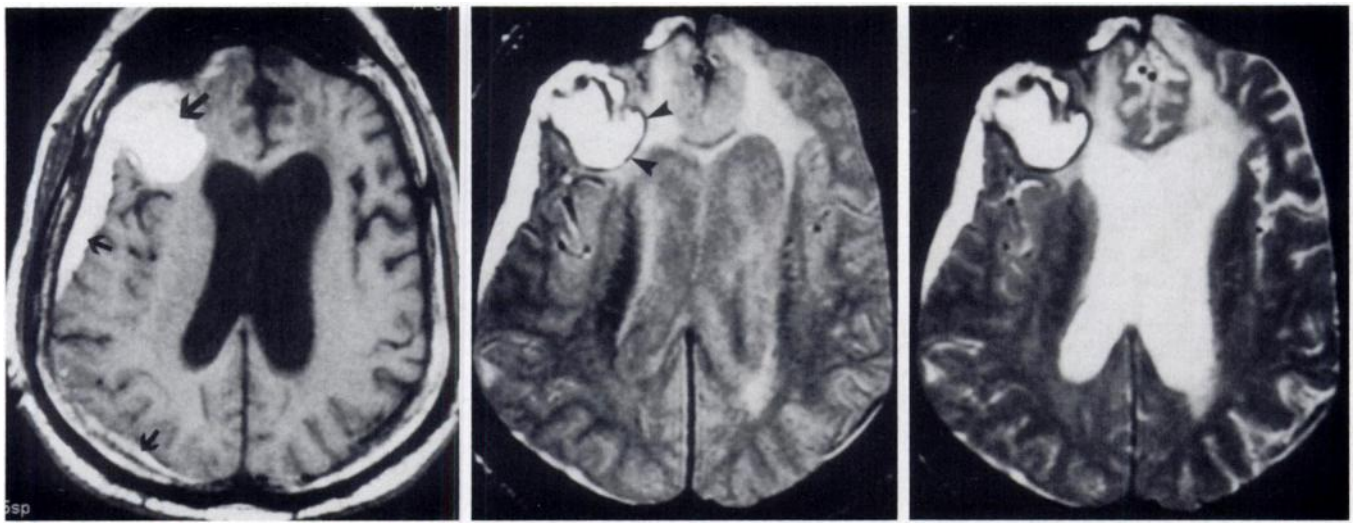

a. b. c.

Figure 9. Late subacute hemorrhage 3 weeks following head trauma to a 64-year-old man. **(a)** T1-weighted (SE 500/20) axial MR image demonstrates high-intensity right convexity subdural hematomas (small arrows), as well as right subfrontal parenchymal hematoma (large arrow). The ventricles are dilated due to associated communicating hydrocephalus from subarachnoid hemorrhage. **(b)** Proton-density–weighted (SE 3,000/20) axial MR image demonstrates persistent hyperintensity of the subdural and parenchymal hematomas relative to lower intensity CSF. A hemosiderin rim (arrowheads) is now becoming visible around the parenchymal hematoma. **(c)** T2-weighted (SE 3,000/80) axial MR image demonstrates persistent hyperintensity of the subdural and parenchymal hematomas, which are now isointense with hyperintense CSF. The combination of high signal intensity on the T1-weighted image with persistent high signal intensity on the T2-weighted image is indicative of extracellular methemoglobin. The hemosiderin rim surrounding the parenchymal hematoma is more apparent with additional T2 weighting, indicating the beginning of the chronic stage.

due to deoxygenation, hemoconcentration, red blood cell dehydration, and/or clot retraction. Further, the relative influence of these factors on T2 shortening depends on the operating field strength (Fig 2) (24).

Early Subacute Phase

The subacute phase is defined by the oxidation of deoxyhemoglobin to methemoglobin (6). In the early subacute phase, the red blood cells are still intact (47). With the formation of methemoglobin, T1 is markedly shortened due to a dipole-dipole interaction, resulting in increased intensity on T1-weighted images (6,47) (Fig 8). For parenchymal hematomas, the formation of methemoglobin begins peripherally (Fig 6) due to "intrinsic tissue factors" (48). In addition, oxygen is needed for the oxidation of the heme iron, and the oxygen level is higher in the normal surrounding brain than in the center of the hematoma. Later, the center becomes oxidized to methemoglobin as well. Interestingly, the pattern of methemoglobin formation is exactly the opposite for partially thrombosed intracranial aneurysms, as the oxygen tension is higher in the central lumen than at the periphery (47).

In the early subacute phase, the red blood cells are still intact. Since methemoglobin is magnetically susceptible, the middle of the red cell becomes more magnetized than the plasma on the outside. Thus, the magnetic nonuniformity that causes T2 shortening with intracellular deoxyhemoglobin persists with intracellular methemoglobin.

T1-weighted imaging is better suited to distinguish acute hemorrhage (long T1) from subacute hemorrhage (short T1). Since methemoglobin has five unpaired electrons (compared to four for deoxyhemoglobin), the T2 of the hematoma should be additionally shortened in the transition from the acute to early subacute phase, although this may be difficult to document.

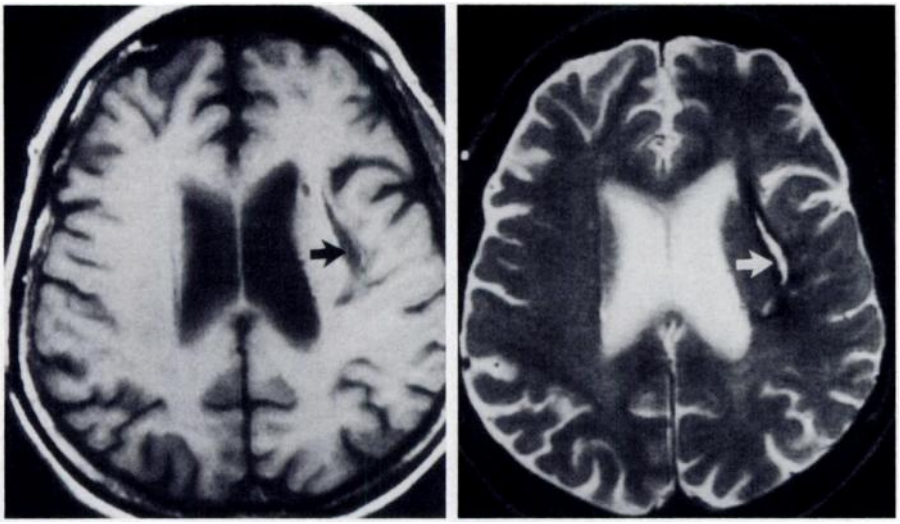

a. b.

Figure 10. Chronic hematoma in a 61-year-old woman who had a documented hemorrhage 9 months previously and now has seizures. **(a)** T1-weighted (SE 500/20) axial MR image demonstrates slitlike encephalomalacia in the high external capsule (arrow). **(b)** T2-weighted (SE 3,000/90) axial MR image demonstrates hemosiderin-lined slit (arrow) from chronic hemorrhage.

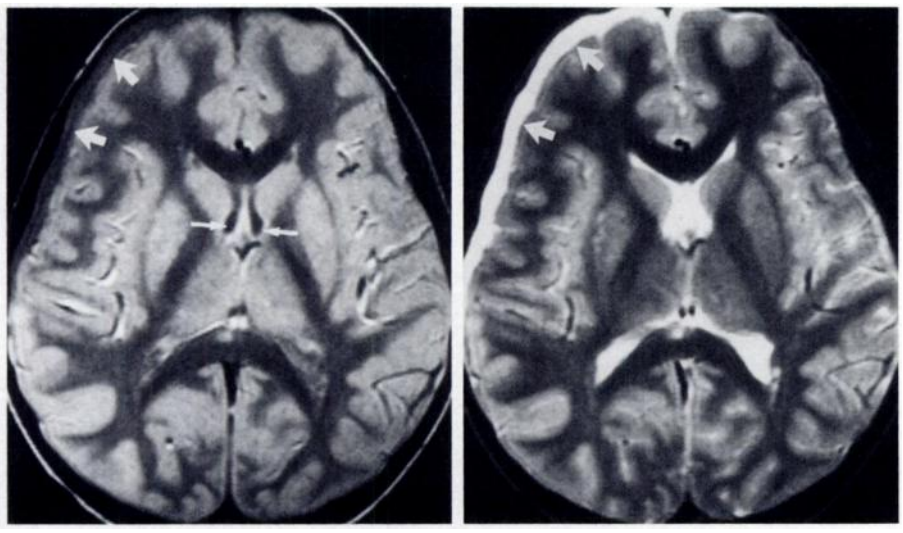

a. b.

Figure 11. Chronic subdural hematoma in a 5-year-old boy 6 months following head trauma. **(a)** So-called proton-density–weighted (SE 3,000/22) MR image demonstrates right convexity subdural hematoma (large arrows) with slightly higher intensity than the CSF in the lateral ventricles (small arrows). The slightly higher signal intensity of the proteinaceous chronic subdural hematoma actually represents T1 shortening from hydration layer water. **(b)** T2-weighted (SE 3,000/90) MR image demonstrates a similar area of high signal intensity in the subdural collection (arrows) and the CSF. On such images, the effects of subtle T1 shortening due to elevated protein concentration are not apparent. (Reprinted, with permission, from reference 7, p 753.)

Late Subacute Phase

Late subacute hemorrhage is bright on *both* T1- and T2-weighted images. By the late subacute phase, red cell lysis has occurred. On T1-weighted images, both early and late subacute hemorrhage appears bright, since water molecules can pass freely across the red blood cell membrane. As lysis occurs, the T2 shortening that had resulted from compartmentalization of methemoglobin is lost (Fig 9). In addition, the high water content of the lysed red cells leads to increase in both T2 and proton density (compared to brain) (49). Obviously, T2-weighted images are necessary for accurate distinction between early (short T2) and late (long T2) subacute hemorrhage (7).

Chronic Phase

In the chronic phase, paramagnetic hemosiderin and ferritin (which have high magnetic susceptibilities) are found within macrophages in a dark rim surrounding the hematoma on T2-weighted images (Fig 9) (30). For ferritin and hemosiderin to be formed, red blood cells containing methemoglobin must first lyse (30). Thus, initially there is always a bright

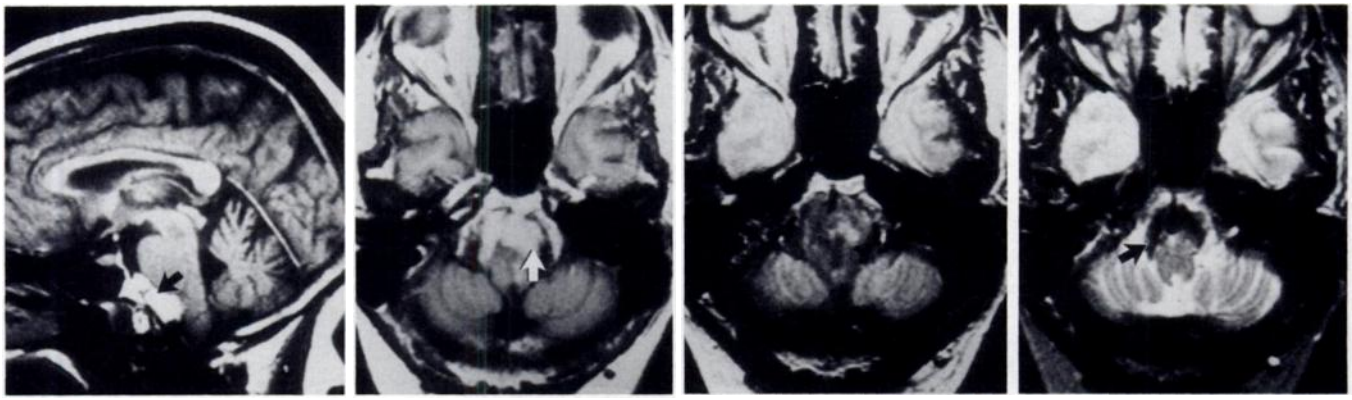

a. b. c. d.

Figure 12. Early subacute subarachnoid hemorrhage in a 32-year-old woman with bleeding from ruptured posterior inferior cerebellar artery aneurysm 2 weeks earlier. **(a)** T1-weighted (SE 450/22) sagittal MR image demonstrates abnormal high signal intensity in the pontine and medullary cisterns (arrow). **(b)** T1-weighted (SE 450/22) axial MR image through the caudal medulla demonstrates abnormal hyperintensity anterior to the brain stem (arrow). **(c)** Proton-density–weighted (SE 3,000/22) axial MR image shows no significant abnormality as the subarachnoid thrombus has become isointense with CSF. **(d)** T2-weighted (SE 3,000/90) axial MR image demonstrates marked hypointensity (arrow) in the subarachnoid thrombus compared to the hyperintense CSF around it. The combination of high signal intensity on the T1-weighted image and low signal intensity on the T2-weighted image is indicative of early subacute hemorrhage.

ring of free methemoglobin just inside the darker hemosiderin ring on T2-weighted images. Eventually the hematoma is reduced to a hemosiderin-lined slit (Fig 10). Like deoxyhemoglobin, intracellular, paramagnetic hemosiderin causes preferential T2 shortening (1).

SUBDURAL AND EPIDURAL HEMATOMAS

Like parenchymal hemorrhage, subdural hematomas have five stages of evolution and thus five different appearances on MR images (7,50,51). Since the dura is so well vascularized, however, the oxygen tension remains high, and the temporal progression from one stage to the next is slower in the extraaxial compartment than in the brain itself (50). The first four stages are the same as for a parenchymal hematoma with the same T1 and T2 characteristics. The chronic stage is characterized by continued oxidative denaturation of methemoglobin, forming nonparamagnetic hemichromes (28). The T1 of such compounds is greater than that of paramagnetic methemoglobin; thus the intensity of chronic subdural hematomas is less than that of subacute subdural hematomas, particularly on T1-weighted images. Chronic subdural hematomas (Fig 11) are less intense than subacute subdural hematomas (Fig 9) but more intense than CSF due to their higher protein content (40,50,51). In the extraaxial compartments during the chronic phase, there is no hemosiderin rim per se because there are no tissue macrophages to surround the hematoma. In the case of recurrent bleeding into a subdural hematoma, however, there may be hemosiderin staining of the membrane, which forms along the inner border of the subdural collection. Like the hemosiderin surrounding a parenchymal hematoma, this will also turn dark on T2-weighted images.

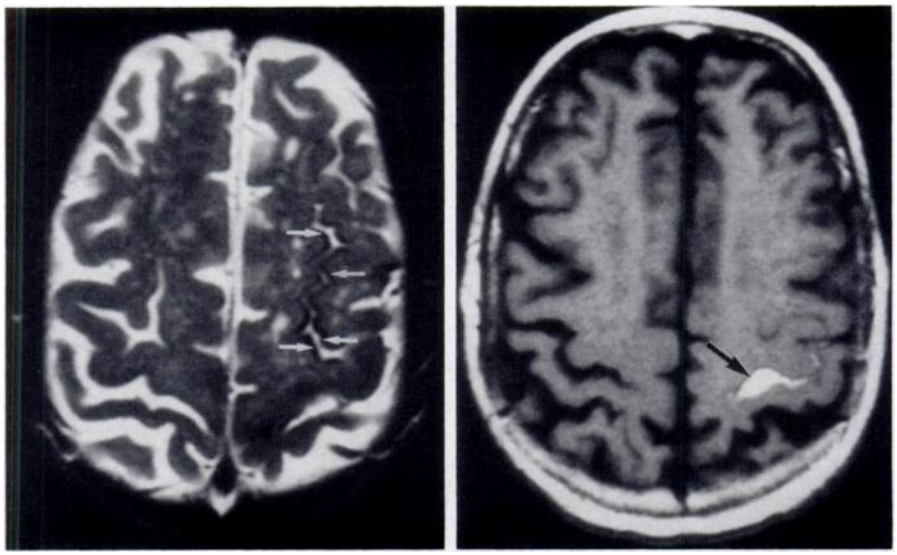

a. b.

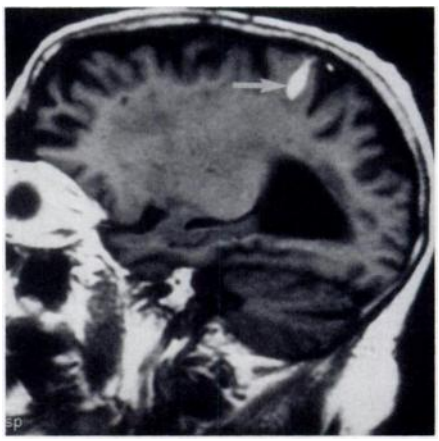

c.

Figure 13. Superficial siderosis in a 65-year-old man following subarachnoid hemorrhage. **(a)** T2-weighted (SE 3,000/80) axial MR image demonstrates linear hypointensity (arrows) involving posterior left frontal gyri due to superficial siderosis from previous subarachnoid hemorrhage. **(b)** T1-weighted (SE 500/20) axial MR image demonstrates methemoglobin within subacute subarachnoid thrombosis in central sulcus (arrow). **(c)** T1-weighted (SE 500/20) left parasagittal MR image demonstrates methemoglobin extending into sulcus (arrow), confirming subarachnoid (vs subdural) location.

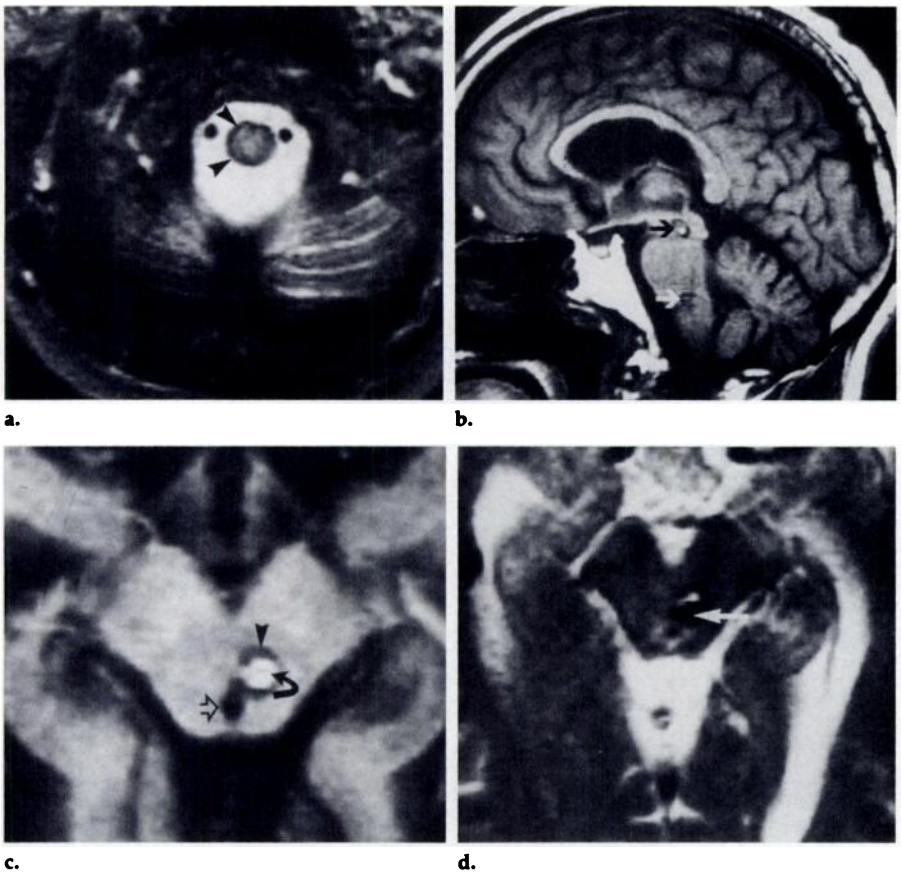

Figure 14. Multiple cavernous angiomas in a 62-year-old Hispanic man with a 1-week history of altered mental status. **(a)** T2-weighted (SE 3,000/90) axial MR section through the upper cervical cord demonstrates linear hypointensity surrounding the cord (arrowheads), secondary to superficial siderosis. **(b)** T1-weighted (SE 500/15) sagittal MR section demonstrates two cavernous angiomas in the brain stem (arrows). **(c)** T1-weighted (SE 500/15) axial MR section through the midbrain lesion demonstrates hemosiderin rim (arrowhead) surrounding methemoglobin (curved arrow) in cavernous angioma adjacent to cerebral aqueduct (open arrow). **(d)** T2-weighted (SE 3,000/90) axial MR image through the same section as **c** demonstrates persistent hemosiderin rim with marked decrease in signal intensity within the cavernous angioma (arrow). The combination of findings indicates that the central hemorrhage is predominantly in the early subacute form and is, therefore, a recent event, correlating with his week-long period of altered sensorium. Multiple cavernous hemangiomas is a familial condition initially described in Hispanics.

In our experience, most elderly patients present in the subacute phase several weeks after the veins bridging the subdural space have been torn by minor trauma. Subdural hematomas are often bilateral and may be of different ages. In this setting, the more intense collection is generally due to the more recent subacute event, while the less intense collection is due to more chronic hemorrhage. When recurrent bleeding occurs in a subdural hematoma, the separate events may be distinguishable by the different signal intensities on MR images.

Epidural hematomas evolve in a manner similar to that of subdural hematomas. They are distinguished from the latter on the basis of classic morphology (ie, bilenticular epidural hematoma vs medially concave subdural hematoma) and by the low intensity of the fibrous dura mater (7) between the hematoma and the brain. Like an acute subdural hematoma, an acute epidural hematoma has deoxyhemoglobin within intact red blood cells, resulting in T2 shortening and low intensity on T2-weighted images, particularly those obtained at high field strength. On the basis of intensity characteristics alone, therefore, it may be difficult to separate the low-intensity dura from the low-intensity hematoma during this phase. In cases of atypical morphology (ie, bilenticular subdural hematoma) it may be difficult to distinguish accurately a subdural from an epidural collection. In the late subacute phase of an epidural hematoma, methemoglobin has been formed and the red cells have lysed, providing excellent contrast between the high-intensity epidural hematoma and the low-intensity dura. Unfortunately, during the late subacute stage of a subdural hematoma with recurrent bleeding, the hemosiderin-stained membrane can simulate the dura, potentially leading to the mistaken diagnosis of epidural hematoma in morphologically atypical cases.

SUBARACHNOID AND INTRAVENTRICULAR HEMORRHAGE

Subarachnoid and intraventricular hemorrhage differs from intraparenchymal, subdural, or epidural hemorrhage in that it is mixed with CSF. Like the extraaxial hematomas, however, subarachnoid and intraventricular hemorrhage have high ambient oxygen levels and thus "age" more slowly than parenchymal hematomas (Fig 12).

Immediately after subarachnoid hemorrhage, there is a small decrease in T1 (6,52–54), reflecting the increase in hydration-layer water (45) due to the higher protein content of the bloody CSF. This leads to subtle increase in signal intensity in the CSF on T1- and proton-density–weighted images ("dirty CSF") (52–54). As has been shown in vitro (6), significant quantities of methemoglobin are not formed until several days after the hemorrhage. Several days to a week after the ictus, signal intensity increases in the subarachnoid space due to methemoglobin formation (Fig 12). In cases of milder subarachnoid hemorrhage, the red blood cells may be resorbed by the time significant methemoglobin formation would have occurred, and, therefore, the anticipated short T1 appearance will not be seen. For these reasons, CT is advocated for the early diagnosis of subarachnoid hemorrhage (6,7). A short T2 appearance is observed in subarachnoid or intraventricular hemorrhage when massive bleeding has occurred, in which case a fluid-fluid level or a subarachnoid or intraventricular *thrombus* may be present (Figs 8, 12) (6,53). In chronic, repeated subarachnoid hemorrhage, hemosiderin may be seen staining the leptomeninges, leading to a short T2 appearance known as "superficial siderosis" (55) (Figs 13, 14).

INTRATUMORAL HEMORRHAGE

Hemorrhage is common in the higher grade gliomas and certain highly vascular metastases, for example, melanoma (Fig 15), choriocarci-

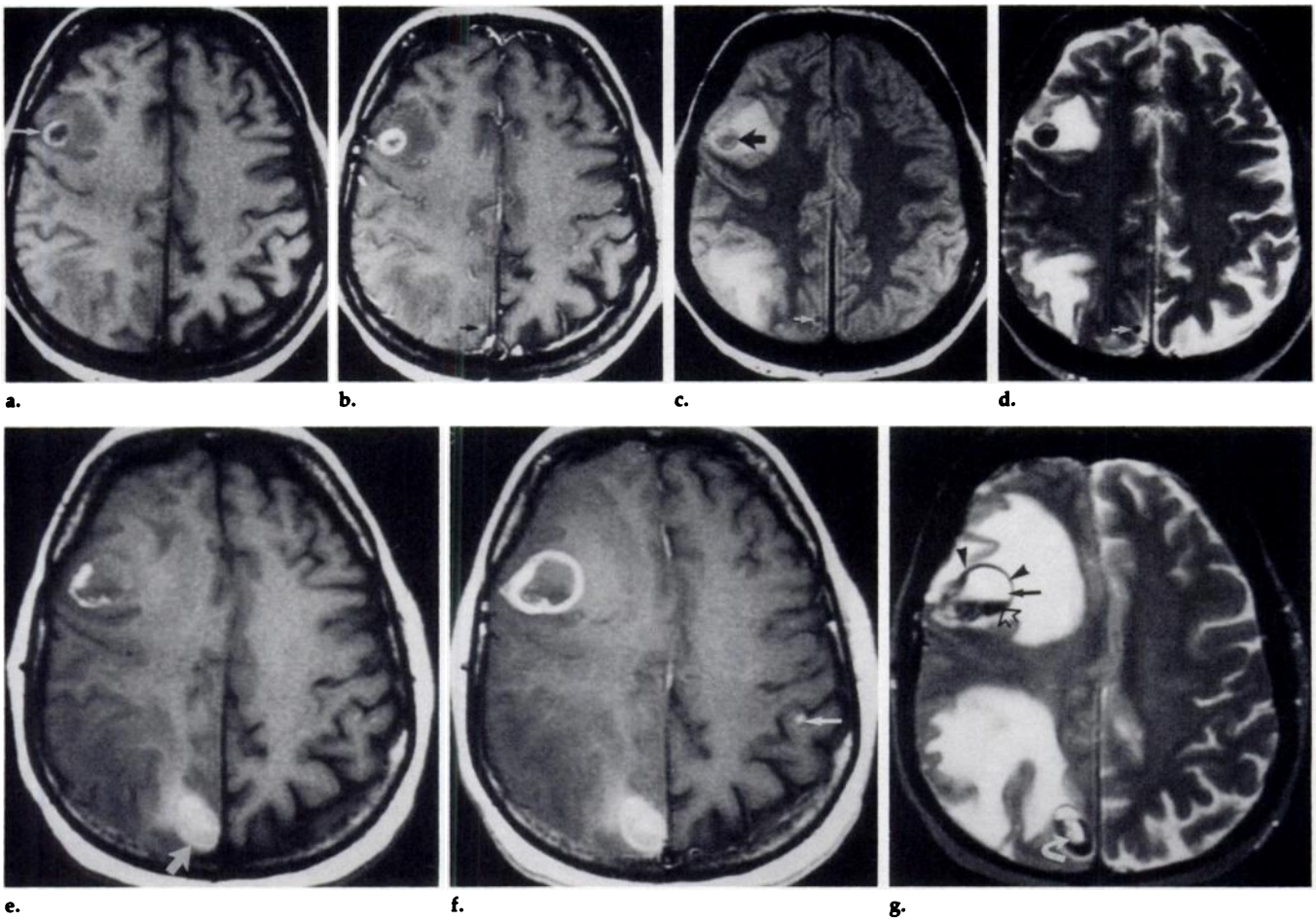

Figure 15. Images of a 46-year-old woman with hemorrhagic metastatic melanoma. **(a)** Unenhanced T1-weighted (SE 500/15) axial MR section demonstrates hyperintensity (arrow) consistent with methemoglobin. **(b)** Gadolinium-enhanced (SE 500/15) axial MR section demonstrates larger area of hyperintensity than noted in **a**, indicating tumoral enhancement. Note also punctate focus of enhancement just anterior to the torcula (arrow), suggestive of possible additional lesion. **(c)** Proton-density–weighted (SE 3,000/22) axial MR image demonstrates edema around right frontal lesion (large arrow), which has now become hypointense, suggesting T2 shortening from hemorrhage. A second, larger area of edema is noted in the right parietal lobe. The punctate focus of enhancement noted in **b** anterior to the superior sagittal sinus now appears hypointense (small arrow). **(d)** T2-weighted (SE 3,000/90) axial MR image demonstrates marked hypointensity and a fluid level in the right frontal lesion. The combination of findings on the unenhanced T1- and T2-weighted images indicates that the marked hypointensity is due to intracellular deoxyhemoglobin centrally with intracellular methemoglobin peripherally. The slightly more intense nondependent portion represents lysed red cells. Note the marked hypointensity of the punctate right parafalcine lesion (arrow) without any evidence of surrounding edema. This is characteristic of hemorrhagic pial metastases. **(e)** Four months later, the follow-up unenhanced MR study (SE 500/20) demonstrates increasing size of all lesions, particularly the posterior right parafalcine lesion (arrow). The hyperintensity of the right frontal and parafalcine is indicative of methemoglobin. **(f)** Gadolinium-enhanced follow-up MR image (SE 500/20) through the same level as **e** demonstrates irregular rim enhancement, particularly of the right frontal lesion, which is indicative of tumor. No definite enhancement is noted in the right parafalcine lesion posteriorly due to the high background signal intensity of the methemoglobin. A new left parietal lesion is also noted (arrow). **(g)** T2-weighted (SE 3,000/90) axial MR image demonstrates fluid levels in both hemorrhagic lesions. The hyperintensity noted in the nondependent position represents serosanguineous fluid (straight solid arrow). The marked hypointensity noted in the dependent position (open arrow) represents a combination of intracellular deoxyhemoglobin centrally and methemoglobin peripherally. The central area of hyperintensity in the posterior right parafalcine lesion (curved arrow), which remains hyperintense on both T1- and T2-weighted images, represents extracellular methemoglobin. Note also the well-defined hemosiderin rim (arrowheads) of the right frontal lesion, which has broken through its lateral margin by recurrent tumor growth (as evidenced by the area of enhancement in **f**).

noma, and carcinoma of the lung, kidney, thyroid, and breast.

The diagnosis of a neoplastic source of hemorrhage may be difficult to make in the subacute setting. Since methemoglobin is already hyperintense, it may be difficult to appreciate marginal gadolinium enhancement against an already intense background. In such cases, CT with and without contrast material may be useful, as the subacute hemorrhage is usually hypoattenuating at CT. (Similarly, during the acute phase of neoplastic hemorrhage, the hyperattenuation at CT may make marginal enhancement difficult to appreciate; simultaneously, the background deoxyhemoglobin on a T1-weighted MR image is hypointense, facilitating the detection of marginal enhancement with gadolinium.)

Early pial metastases are notoriously difficult to detect without gadolinium, due to the lack of associated vasogenic edema and T2 prolongation (56). Should these metastases be hemorrhagic (Fig 15), they may actually be hypointense on T2-weighted images due to intracellular deoxyhemoglobin and methemoglobin.

Whether a hematoma results from a tumor or other source, fluid-fluid levels may be seen. The dependent portion is often hypointense on T2-weighted images due to the presence of intact red blood cells containing deoxyhemoglobin or methemoglobin. The nondependent fluid is more intense than CSF on proton-density– and T2-weighted images but not as intense as methemoglobin on T1-

weighted images. These signal intensity characteristics are indicative of mild T1 shortening due to the proteinaceous serosanguineous serum (40).

When followed sequentially, intratumoral hemorrhage may appear to evolve more slowly than parenchymal hematomas, reflecting the much lower ambient oxygen levels (57). Delayed evolution of hematomas is, therefore, seen both in the setting of low O_2 (not enough to oxidize the heme iron from ferrous deoxyhemoglobin to ferric methemoglobin) and high O_2 (which keeps the methemoglobin reductase systems powered to drive methemoglobin back to deoxyhemoglobin). The optimal O_2 tension for hemoglobin oxidation is approximately 20 mm Hg (58).

When tumors bleed in the brain, macrophages move in to surround the hemorrhage just as in the nonneoplastic situation. Hemosiderin or ferritin rims are seen in the chronic setting. With renewed tumor growth, the hemosiderin rim may become disrupted (47) (Fig 15). While this is a useful sign of neoplastic hemorrhage, it is less than 100% specific because rebleeding from any cause—for example, hypertension—can produce disruption of an earlier hemosiderin rim.

SUMMARY

Although CT may be more useful for detecting hyperacute parenchymal hemorrhage or early subarachnoid or intraventricular hemorrhage, MR is certainly more sensitive after 12–24 hours. MR is also more specific than CT in determination of the age of the hemorrhage. Hemorrhage passes through five well-defined and easily identified stages on MR images as it evolves. Knowledge of these stages may be useful to date a single hemorrhagic event or to suggest that multiple hemorrhagic events have occurred at different times. As stressed throughout this review, it is important to acquire *both* T1- and T2-weighted images to adequately characterize and stage hemorrhage. ■

Acknowledgments: I thank Michael McCurdy, Diane Savala Pinkerman, Lisa Slocum, Lillian Cayetano, Venita Lombard-Smith, Dorothy Pizano, and Terry Robey for technical assistance; Janet Cegnar, MD, for help in case selection; Dana Murakami, MD, for manuscript review; and Kaye Finley for manuscript editing and preparation.

References

1. Gomori JM, Grossman RI, Goldberg HI, et al. Intracranial hematomas: imaging by high field MR. Radiology 1985; 157:87–92.
2. DeLaPaz RL, New PFL, Buonanno FS, et al. NMR imaging of intracranial hemorrhage. J Comput Assist Tomogr 1983; 8:599–607.
3. Sipponen JT, Sepponen RE, Sivula A. Nuclear magnetic resonance (NMR) imaging of intracerebral hemorrhage in the acute and resolving phases. J Comput Assist Tomogr 1983; 7:954–959.
4. Hayman LA, Pagan JJ, Kirkpatrick JB, Hinck VC. Pathophysiology of acute intracerebral and subarachnoid hemorrhage: applications to MR imaging. AJNR 1989; 10:457–481.
5. Brooks RA, DiChiro G, Patronas N. MR imaging of cerebral hematomas at different field strengths: theory and applications. J Comput Assist Tomogr 1989; 13:194–206.
6. Bradley WG, Schmidt PC. Effect of methemoglobin formation on the MR appearance of subarachnoid appearance. Radiology 1985; 1156:99–103.
7. Bradley WG. Hemorrhage and brain iron. In: Stark DD, Bradley WG, eds. Magnetic resonance imaging. 2nd ed. St Louis, Mo: Mosby–Year Book, 1992.
8. Zyed AM, Hayman LA, Bryan RN. MR imaging of intracerebral blood: diversity in the temporal pattern at 0.5 and 1.0 T. AJNR 1991; 12:469–474.
9. Zimmerman RD, Heier LA, Snow RD, Liu DPC, Kelly AB, Deck MDF. Acute intracranial hemorrhage: intensity changes on sequential MR scans at 0.5 T. AJNR 1988; 9:47–57.
10. Zimmerman RD, Deck MDF. Intracranial hematomas: imaging by high field MR (letter). Radiology 1986; 159:565.
11. Fullerton GD. Physiologic basis of magnetic relaxation. In: Stark DD, Bradley WG, eds. Magnetic resonance imaging 2nd ed. St Louis, Mo: Mosby-Year Book, 1992; 88–108.
12. Bradley WG. Hemorrhage and vascular abnormalities. In: Bradley WG, Bydder GM, eds. MRI atlas of the brain. London, England: Dunitz, 1990; 201–264.
13. Bloembergen N, Purcell EM, Pound RV. Relaxation effects in nuclear magnetic resonance absorption. Phys Rev 1948; 73:679–712.
14. Atlas SW, Mark AS, Grossman RI, Gomori JM. Intracranial hemorrhage: gradient-echo MR imaging at 1.5 T—comparison with spin-echo and clinical applications. Radiology 1988; 168:803–807.
15. Mills TC, Ortendahl DA, Hylton NM, et al. Partial flip angle MR imaging. Radiology 1987; 162:531–539.
16. Hardy PA, Kucharczyk W, Henkelman RM. Cause of signal loss in MR images of old hemorrhagic lesions. Radiology 1990; 174: 549–555.
17. Edelman RR, Johnson K, Buxton R, et al. MR of hemorrhage: a new approach. AJNR 1986; 7:751–756.
18. Seidenwurm D, Meng TK, Kowalski HK, Weinreb JC, Kricheff II. Intracranial hemorrhagic lesions: evaluation with spin-echo and gradient-refocused MR imaging at 0.5 and 1.5 T. Radiology 1989; 172:189–194.
19. Wesbey GE, Moseley ME, Ehman RL. Translational molecular self-diffusion in magnetic resonance imaging: effects and applications" In: James TL, Margulis AR, eds. Biomedical magnetic resonance. San Francisco, Calif: University of California Press, 1984; 63–76.
20. Packer KJ. The effects of diffusion through locally inhomogeneous magnetic fields on transverse nuclear spin relaxation in heterogeneous systems: proton transverse relaxation in striated muscle tissue. J Magn Reson 1973; 9:438–443.
21. Feinberg DA, Oshio K. GRASE (gradient- and spin-echo) MR imaging: a new fast clinical imaging technique. Radiology 1991; 181:597–602.
22. Norbash AM, Glover GH, Enzmann DR. Intracerebral lesion contrast with spin-echo and fast spin-echo pulse sequences. Radiology 1992; 185:661–665.
23. Jones KM, Mulkern RV, Mantello MT, et al. Brain hemorrhage: evaluation with fast spin-echo and conventional dual spin-echo images. Radiology 1992; 182:53–58.
24. Clark RA, Watanabe AT, Bradley WG, Roberts JD. Acute hematomas: effects of deoxyhemoglobin, hematocrit, and fibrin-clot formation and retraction on T2 shortening. Radiology 1990; 174:201–206.
25. Hayman LA, McArdle C, Taber K, et al. MR imaging of hyperacute intracranial hemorrhage in the cat. AJNR 1989; 10:681–686.
26. Hayman LA, Ford JJ, Taber KH, Saleem A, Round ME, Bryan RN. T2 effect of hemoglobin concentration: assessment with in vitro MR spectroscopy. Radiology 1988; 168:489–491.
27. Hayman AL, Taber KH, Ford JJ, et al. Effect of clot formation and retraction on spin-echo MR images of blood: an in vitro study. AJNR 1989; 10:1155–1158.
28. Wintrobe MM, Lee GR, Boggs DR, et al. Clinical hematology Philadelphia, Pa: Lea & Febiger, 1981; 88–102.
29. Rapoport SI. Introduction to hematology. New York, NY: Harper & Row, 1971; 31.
30. Thulborn KR, McKee A, Kowall NW, et al. Role of ferritin and hemosiderin in the MR appearance of cerebral hemorrhage: a histopathologic biochemical study in rats. AJNR 1990; 11:291–297.
31. Faraday M. Cited by: Pauling L, Coryell C. The magnetic properties and structure of hemoglobin, oxyhemoglobin, and carbonmonoxyhemoglobin. Proc Natl Acad Sci 1936; 22:210–216.
32. Pauling L, Coryell C. The magnetic properties and structure of the hemochromogen and related substances. Proc Natl Acad Sci 1936; 22:159–163.
33. Koenig SH, Brown RD, Linstrom TR. Interactions of solvent with the heme region of methemoglobin and fluoromethemoglobin. Biophys J 1981; 34:397–408.
34. Singer JR, Crooks LE. Some magnetic studies of normal and leukemic blood. J Clin Eng 1978; 3:357–363.
35. Zimmerman RD, Heier LA, Snow RB, Liu DPC, Kelly AB, Deck MDF. Acute intracranial hemorrhage: intensity changes on sequential MR scans at 0.5 T. AJNR 1988; 9:47–57.
36. Bradley WG. Hemorrhage and brain iron. In: Stark DD, Bradley WG, eds. Magnetic resonance imaging. St Louis, Mo: Mosby–Year Book, 1988; 721–769.
37. Whisnant JP, Sayer GP, Millikan CH. Experimental intracerebral hematoma. Arch Neurol 1963; 9:586–592.
38. Bydder GM, Payne JA, Collins AF, et al. Clinical use of rapid T2-weighted partial saturation sequences in MR imaging. J Comput Assist Tomogr 1987; 11:17–26.
39. Rapoport S, Sostman HD, Pope C, et al. Venous clots: evaluation with MR imaging. Radiology 1987; 162:527–530.
40. Fullerton GD, Cameron IL, Ord VA. Frequency dependence of magnetic resonance spin lattice relaxation of protons in biological materials. Radiology 1984; 151:135–138.
41. Fullerton GD, Finnie MF, Hunter KE, et al. The influence of macromolecular polymerization on spin lattice relaxation of aqueous solutions. Magn Reson Imaging 1987; 5:353–370.
42. Alanen A, Kormano M. Correlation of the

echogenicity and structure of clotted blood. J Ultrasound Med 1985; 4:421–425.
43. Chin HY, Taber KH, Hayman LA, Ford JJ, Kirkpatrick JB. Temporal changes in red blood cell hydration: application to MRI of hemorrhage. Neuroradiology 1991; 33(suppl):79–81.
44. Enzmann DR, Britt RH, Lyons BE, Buxton JL, Wilson DA. Natural history of experimental intracerebral hemorrhage: sonography, computed tomography and neuropathology. AJNR 1981; 2:517–526.
45. Fabry ME, Eisenstadt M. Water exchange across red cell membranes. II. Measurement by nuclear magnetic resonance T1, T2, and T12 hybrid relaxation: the effects of osmolarity, cell volume and medium. J Membr Biol 1978; 42:375–398.
46. Taber KH, Ford JJ, Jensen RS, et al. Change in red blood cell relaxation with hydration: application to MR imaging of hemorrhage. JMRI 1992; 2:203–208.
47. Gomori JM, Grossman RI. Head and neck hemorrhage. In: Kressel HY, ed. Magnetic resonance annual. New York, NY: Raven, 1987; 71–112.
48. Taber KH, Miglior PJ, Pagani JJ, Ford JJ, McLauren T, Hayman LA. Temporal changes in the oxidation state in vitro blood. Invest Radiol 1990; 25:240–244.
49. Hackney DB, Atlas SW, Grossman RI, et al. Subacute intracranial hemorrhage: contribution of spin density to appearance on spin-echo MR images. Radiology 1987; 165: 199–202.
50. Fobben ES, Grossman RI, Atlas SW, et al. MR characteristics of subdural hematomas and hygromas at 1.5 T. AJNR 1989; 10:687–696.
51. Ebisu T, Naruse S, Horikawa Y, Tanaka C, Higuchi T. Nonacute subdural hematoma: fundamental interpretation of MR images based on biochemical and in vitro MR analysis. Radiology 1990; 171:449–453.
52. Chakeres DW, Bryan RN. Acute subarachnoid hemorrhage: in vitro comparison of magnetic resonance and computed tomography. AJNR 1987; 7:223–228.
53. Yoon HC, Lufkin RB, Vinuela F, et al. MR of acute subarachnoid hemorrhage. AJNR 1988; 9:405–408.
54. Satoh S, Kadoya S. Magnetic resonance imaging of subarachnoid hemorrhage. Neuroradiology 1988; 30:361–366.
55. Gomori J, Grossman RI, Bilaniuk LT, et al. High field MR imaging of superficial siderosis of the central nervous system. J Comput Assist Tomogr 1985; 9:972–975.
56. Paakko E, Patronas NJ, Schellinger D. Meningeal Gd-DTPA enhancement in patients with malignancies. J Comput Assist Tomogr 1990; 14:542–550.
57. Destian S, Sze G, Krol G, Zimmerman RD, Deck MD. MR imaging of hemorrhagic intracranial neoplasms. AJR 1989; 152:137–144.
58. Kelly WM, Johnson BA. Understanding intracranial hemorrhage: a practical approach. MRI Decisions 1993; 7:9–22.